Palestinian Medical and Pharmaceutical Journal

Synthesis and Enzymatic Hydrolysis Study of Acyloxyalkyl Carbamate as New Prodrug for Amine

Israa Abad Alrasol Mohamed Sadeq[1,*], Mohammed Dheyaa Al-Ameedee[1] & Ali Rasool Mahmood Albakaa[1]

(Type: Full Article). Received: 5th Dec. 2024, Accepted: 3rd Mar. 2025, Published: 1st Mar. 2026,
DOI: https://doi.org/10.59049/2790-0231.11.1.2422

Abstract: Fluoxetine is an antidepressant classified as a selective serotonin reuptake inhibitor (SSRI). Its bioavailability is low due to its varying dissolution at different pH levels and rapid breakdown in the liver. To address these challenges, a series of five novel fluoxetine derivatives (A1–A5) were synthesized by introducing various acyloxyalkyl carbamate groups at the fluoxetine amino moiety. The structural integrity and chromatographic purity of these derivatives were confirmed through Fourier-transform infrared (FT-IR) spectroscopy, proton nuclear magnetic resonance (^{1}H-NMR), and carbon-13 nuclear magnetic resonance (^{13}C-NMR) analyses. The enzymatic hydrolysis rates were assessed using ultraviolet-visible (UV-Vis) spectroscopy (λmax: 227 nm) in human plasma, revealing controlled-release profiles modulated by the steric bulk of the acyloxyalkyl substituents. At 120 minutes, the hydrolysis rates were as follows: A1 (99.5%), A2 (97.0%), A3 (96.9%), A4 (95.0%), and A5 (94.5%). These results highlight the potential of the acyloxyalkyl carbamate moiety to enhance drug absorption, reduce adverse effects, and improve therapeutic outcomes. The study demonstrates the feasibility of addressing fluoxetine's pharmacokinetic limitations through prodrug design. Future research should focus on comprehensive *in vivo* investigations to validate the *in vitro* findings and evaluate these derivatives' long-term pharmacokinetics, biological efficacy, and safety.

Keywords: Fluoxetine Prodrug, Acyloxy Alkyl Carbamate, Enzyme-Triggered Release, Esterase Activation, Pharmacokinetic.

Introduction

Major depressive disorder (MDD) is one of the most common and severe mental health illnesses. It affects roughly 15% of the world's population, with women experiencing much greater rates than males [1, 2]. Due to suicide or other concurrent medical illnesses such as cardiovascular diseases, MDD has a significant risk of early mortality [3, 4]. Significant deficits in productivity and day-to-day functioning are another outcome of the disease. In basic care settings, depression is frequently underdiagnosed and untreated, despite being curable [5].

The World Health Organization lists chronic sorrow, loss of interest or pleasure, irregular hunger, guilt, low self-esteem, exhaustion, and trouble concentrating as some of the symptoms of depression [6]. Significant functional impairments may result from this condition, which can be chronic or recurrent [7]. Some subgroups of depression, such as seasonal, psychotic, and melancholic depression, are included in the classification and may react differently to medication [8].

Selective serotonin reuptake inhibitors (SSRIs), such as fluoxetine, are among the most often prescribed antidepressants in use today [9, 10]. Since it selectively targets serotonin reuptake transporters, fluoxetine—one of the first SSRIs to be licensed by the FDA in 1987 [11]—remains a top choice for treating depression [12, 13]. On the other hand, problems with its pH-dependent solubility and hepatic first-pass metabolism can make it less bioavailable and cause a delay in the start of treatment when taken orally [14, 15].

Fluoxetine has significant adverse effects, drug-drug interactions, and contraindications despite its efficacy. Sexual dysfunction, headaches, nausea, and sleeplessness are typical adverse effects. When taken with other serotonergic medications, there are serious hazards, including serotonin syndrome. Careful monitoring is necessary for drug-drug interactions, especially those involving pimozide and monoamine oxidase inhibitors (MAOIs). Hypersensitivity to fluoxetine and concurrent use with specific drugs are examples of contraindications. [16]. The synthesis of many derivatives targeted at improving pharmacokinetics, reducing side effects, and increasing patient outcomes is the result of efforts to improve the therapeutic profile of fluoxetine. Prodrug approaches have been investigated to overcome drawbacks including pH-dependent solubility and hepatic first-pass metabolism. These changes have demonstrated potential for enhancing therapeutic efficacy and bioavailability [17].

This work focuses on adding different acyloxyalkyl carbamate groups to create a new class of fluoxetine derivatives (A1–A5). These compounds are intended to circumvent the pharmacokinetic constraints of conventional fluoxetine and provide controlled-release characteristics. To determine the new derivatives' potential for therapeutic use, the research aims to synthesize them, characterize their structures, and measure their enzymatic hydrolysis rates.

Prodrugs are inactive compounds designed to convert into active drugs after administration, enhancing pharmacokinetics and reducing side effects [19–22]. They improve bioavailability, inhibit first-pass metabolism, and reduce gastrointestinal degradation, addressing fluoxetine's limitations [15, 16]. Prodrugs are classified into bioprecursor and carrier-linked types. Carrier-linked prodrugs release the active drug via enzymatic cleavage [23], while bioprecursors are activated through the metabolic transformation without a carrier [24–26].

Prodrugs' hydrolysis rates, influenced by their chemical makeup and the enzymes that aid in the conversion process,

1 Department of Pharmaceutical Chemistry, Faculty of Pharmacy, Mustansiriyah University, Baghdad, Iraq.
* Corresponding author email: esraa_abdul_rasoul@uomustansiriyah.edu.iq

play a major role in determining their effectiveness. Ester linkages are broken via enzymatic hydrolysis, frequently aided by esterases to liberate the active ingredient. The rate of this conversion can strongly impact the prodrug's ability to be therapeutically efficacious. It is essential to comprehend the impact of varying acyl group sizes on hydrolysis rates when creating prodrugs with regulated release profiles [25]. Using butyrylcholinesterase as a model enzyme, this study examines the effect of acyl group size on hydrolysis rates, which aids in optimizing prodrug design. We hope to offer important insights into creating prodrugs with enhanced therapeutic efficacy by investigating these interactions [24].

Amines are present in many pharmacologically active medications, and prodrug techniques can increase their lipid solubility and membrane permeability [27]. For primary and secondary amine medications, the (acyloxy) alkyl carbamylation technique improves lipophilicity, metabolic stability, and chemical stability [28–30]. The non-ionizable character of (acyloxy)alkoxy promoieties at physiological pH, their simplicity of synthesis, and their enzyme-triggered release make them particularly valuable as prodrugs [31]. However, because of stereochemical variations, the chiral amines used in this method may show varying hydrolysis rates [32–34].

Because of their stability and ability to cross biological membranes, carbamate-containing medications are an important structural class frequently utilized in medicinal chemistry as peptide bond replacements [35, 36]. Since carbamates in prodrugs are bioreversible and can improve drug distribution, they are engineered to release the parent amine upon hydrolysis, which is mediated by esterases [37–39]. Their rate of hydrolysis is an important factor in determining how long the therapeutic action lasts and how effective it is [39]. This research is significant in enhancing the pharmacokinetic properties of fluoxetine through the strategic design of prodrugs. Despite the clinical utility of fluoxetine as an antidepressant, its effectiveness is often compromised by issues related to solubility and bioavailability. The innovative approach of developing prodrugs aims to overcome these barriers, thereby facilitating improved absorption and distribution within biological systems. Such advancements not only have the potential to optimize therapeutic outcomes for patients with depression but also contribute to the broader field of pharmaceutical sciences by addressing critical challenges in drug delivery and efficacy. The research objectives are delineated following this contextual framework, ensuring a clear understanding of the study's aims.

Materials and Methods

Materials

Fluoxetine and isobutyric acid were procured from Hyperchem (China). Propanoic acid and chloroethyl chloroformate were obtained from Loba Chemie (India) and Flourochem (UK), respectively. Benzoic acid was supplied by Srlchem (India), while glacial acetic acid was provided by Macron Fine Chemicals (USA). Pyridine and chloroform were acquired from Thomas Baker (India), and salicylic acid was sourced from Pure Chem (India). Silver monoxide was supplied by Alpha Chemika (India). Sodium hydroxide was obtained from BDH (England), and dioxane was supplied by Loba Chemie (India).

Equipment

Stuart electrical melting point equipment (UK) was used for melting point determination. A Japanese Shimadzu 8400S spectrophotometer was used for the FT-IR analysis. The 1H-NMR and 13C-NMR spectra were recorded using a Bruker Avance NEO spectrometer (400 MHz for ^{1}H-NMR and 100 MHz for ^{13}C-NMR, Germany). A Shimadzu UV-Vis spectrophotometer (Japan) was used for 200–400 nm UV analysis.

Chemical synthesis

The overall chemical synthesis conditions and the approach for the preparation of fluoxetine prodrug derivatives are illustrated in Scheme (1) below.

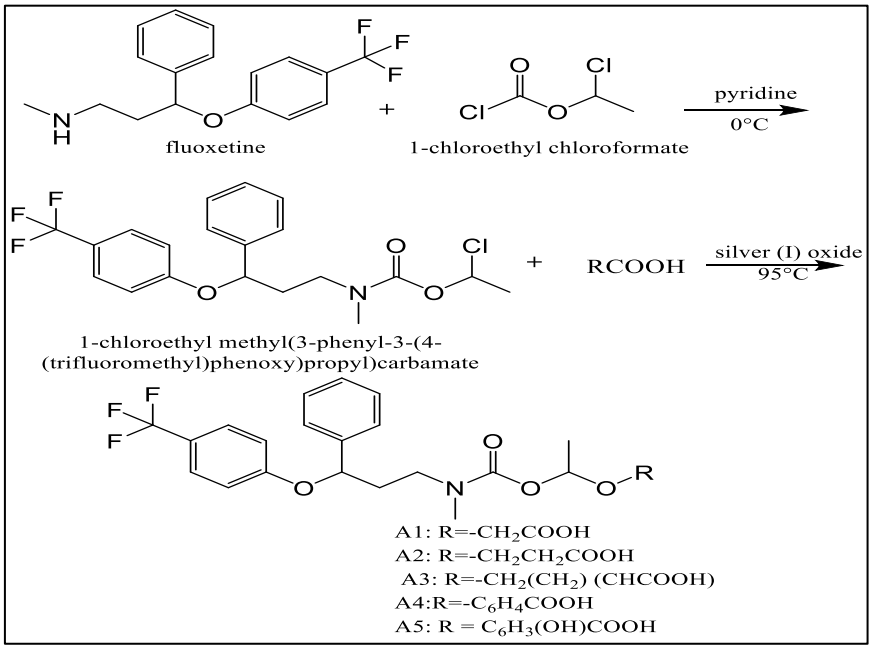

Scheme (1): Synthesis of acyloxy alkyl carbamate prodrug of fluoxetine.

General synthesis of acyloxyalkylcarbamate fluoxetine derivatives (A1-A5)

At 0°C, 40 µL of pyridine and 1.2 mmol of 1-chloroethyl chloroformate were gradually added to a solution of fluoxetine (1 mmol) in 5 mL of chloroform, the reaction mixture was stirred at room temperature. The crude carbamate derivative was obtained and utilized immediately in the following step without any purification. The carbamate derivative was combined with a specific organic acid in the esterification step to prepare different derivatives of the prodrug. Acetic acid was used for A1, propanoic acid for A2, isobutyric acid for A3, benzoic acid in

dioxane for A4, and salicylic acid in dioxane for A5. The reaction mixture was heated to 75°C, followed by the addition of silver (I) oxide. The temperature was then raised to 95°C, and the mixture was stirred for three hours. Following the completion of the reaction, sodium carbonate was used to neutralize the excess of organic acid. The silver oxide was removed by filtration. The final product was separated and purified from the reaction mixture by liquid-liquid extraction method using a 1:1 chloroform/ water mixture was effective in achieving pure compounds, as evidenced by the clear and well-resolved signals in the FT-IR,1H-NMR, and 13C-NMR spectra. The chemical structures of acyloxy alkyl carbamate derivatives (A1–A5) and their chemical names are shown in table (1).

Table (1): Chemical structures of acyloxyalkylcarbamate derivatives (A1–A5) and their chemical names.

COMP.	STRUCTURE	IUPAC NAME
A1	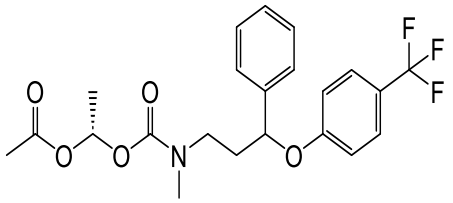	[1S]-1-[[methyl[3-phenyl-3-[4-[trifluoromethyl]phenoxy]propyl]carbamoyl]oxy]ethyl acetate
A2	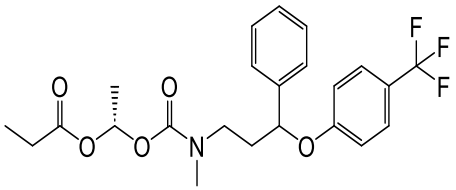	[1S]-1-[[methyl[3-phenyl-3-[4-[trifluoromethyl]phenoxy]propyl]carbamoyl]oxy]ethyl propionate
A3	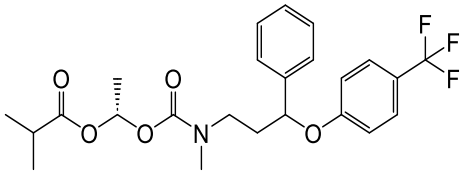	[1S]-1-[[methyl[3-phenyl-3-[4-[trifluoromethyl]phenoxy]propyl]carbamoyl]oxy]ethyl isobutyrate
A4	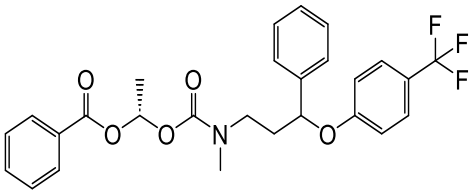	[1S]-1-[[methyl[3-phenyl-3-[4-[trifluoromethyl]phenoxy]propyl]carbamoyl]oxy]ethyl benzoate
A5	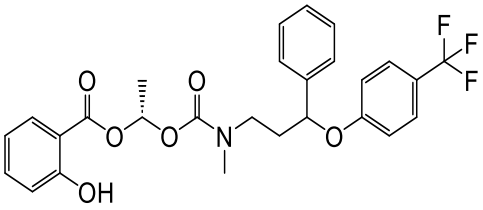	[1S]-1-[[methyl[3-phenyl-3-[4-[trifluoromethyl]phenoxy]propyl]carbamoyl]oxy]ethyl 2-hydroxybenzoate

Synthesis of compound (A1) (1S)-1-((methyl (3-phenyl-3-(4-(trifluoromethyl) phenoxy) propyl)carbamoyl)oxy)ethyl acetate

Physical appearance: faint yellow powder, yield: 89%. Melting point: 193-198ºC. FT-IR: 1022.31 cm^{-1} (C-F stretching vibration characteristic of the CF_3 group), 1116.82 cm^{-1} (stretching vibration associated with the ether group), 1166.97 cm^{-1} (C-O stretching vibration found in the ester group), 1251.84 cm^{-1} (C-O stretching vibration within the carbamate group), 1415.80 cm^{-1} (bending vibration related to CH_3 groups), 1562.39 cm^{-1} (C=C stretching vibration typical of aromatic rings), 1639.55 cm^{-1} (C=O stretching vibration specific to the carbamate group), 1705.13 cm^{-1} (C=O stretching vibration attributed to the ester group), 2931.90, 3001.34 cm^{-1} (stretching vibration of CH_3 groups in alkanes), and 3000–3100 cm^{-1} (C-H stretching vibration associated with aromatic rings). ^{1}H-NMR (DMSO-d_6, 400 MHz), δ (ppm): 1.71 (d, 3H, proton CH_3), 2.28 (q, 2H, proton CH_2), 2.51 (m, 2H, proton CH_2), 2.60 (t, 2H, CH_2 attached to N atom), 4.42 (s, 3H, CH_3 attached to N atom), 5.54 (triblet, 1H, CH of benzylic proton), 7.05 – 7.07 (d, 2H, CH proton of aromatic ring A), 7.24 – 7.26 (m, 2H, CH proton of aromatic ring B), 7.28 – 7.33 (t, 1H, CH proton of aromatic ring B), 7.35 – 7.39 (d, 2H,CH proton of aromatic ring B), 7.41 – 7.46 (t, 2H, CH of aromatic ring A), 7.54 – 7.56 (q, 2H, proton of O-CH-O). ^{13}C-NMR (DMSO-d_6,100 MHz), δ (ppm): 20.72 (CH_3), 29.18 (CH_3), 29.51 (CH_2), 30.27 (CH_3), 55.57 (CH_2), 83.92 (CH-O), 98.18 (O-CH-O), 106.18 (C in aromatic ring A), 113.60 (C in aromatic ring A), 126.33 (C bonded to the trifluoride group), 127.15 (CH in aromatic ring B), 128.13 (CH in aromatic ring A), 129.25 (CH in aromatic ring B), 133.20 (CH in aromatic ring B), 142.98 (C in aromatic ring B), 168.73 (C=O), 176.51 (C in aromatic ring), 184.07 (C=O).

Synthesis of compound (A2) (1S)-1-((methyl (3-phenyl-3-(4-(trifluoromethyl) phenoxy) propyl)carbamoyl)oxy)ethyl propionate

Physical appearance: faint yellow sticky powder. Yield: 82%. Melting point: 182-188ºC. FT-IR: 1022.31 cm^{-1}, 1058.96 cm^{-1} (C-F stretching vibrations in the CF_3 group), 1116.82 cm^{-1} (vibrations associated with the ether group), 1166.97 cm^{-1} (C-O stretching vibrations characteristic of the ester group), 1251.84 cm^{-1} (C-O stretching vibrations in the carbamate group), 1415.80 cm^{-1} (CH_3 group bending vibrations), 1562.39 cm^{-1} (C=C stretching vibrations in aromatic rings), 1639.55 cm^{-1} (C=O stretching vibrations typical of the carbamate group), 1705.13 cm^{-1} (C=O stretching vibrations of the ester group), 2931.90 cm^{-1}, 3001.34 cm^{-1} (CH_3 group stretching vibrations in alkanes), and 3100 cm^{-1} (C-H stretching vibrations in aromatic rings).. ^{1}H-NMR (DMSO-d_6, 400 MHz), δ (ppm): 0.94 – 0.95 (t, 3H, proton of CH_3), 2.11 – 2.12 (d, 3H, proton of CH_3), 2.80 – 2.82 (q, 2H, proton of CH_2), 2.30 (m, 2H, proton of CH_2), 2.96 (t, 2H, CH_2 attached to N atom), 4.75 (s, 3H, CH_3 attached to N atom), 5.71 (triblet, 1H,CH proton of benzylic), 7.07 – 7.09 (d, 2H, CH proton of aromatic ring A), 7.24 – 7.26 (m, 2H, CH proton of aromatic ring B), 7.28 – 7.33 (t, 1H, CH proton of aromatic ring B), 7.35 – 7.37 (d, 2H, CH proton of aromatic ring B), 7.42 – 7.44 (t, 2H, CHproton of aromatic ring A), 7.53 – 7.55 (q, 2H, proton of O-CH-O).^{13}C- NMR (DMSO-d_6,100MHz),δ (ppm): 9.94 (CH_3), 20.72 (CH_3), 29.18 (CH_2), 29.51 (CH_2), 30.27 (CH_3), 44.57 (CH_2), 87.66 (CH-O), 92.08 (O-CH-O), 106.18 (C in aromatic ring A, 2C), 118.97 (C in aromatic ring A), 126.33 (C bonded to trifluoride group), 127.15 (CH in aromatic ring B), 128.13 (CH in aromatic ring A, 2C), 129.25 (CH in aromatic ring B, 2C), 133.20 (CH in aromatic ring B, 2C), 142.98 (C in aromatic ring B), 153.58 (C=O), 157.23 (C=O), 168.73 (C in aromatic ring).

Synthesis of compound (A3) (1S)-1-((methyl (3-phenyl-3-(4-(trifluoromethyl) phenoxy) propyl) carbamoyl) oxy) ethyl isobutyrate

Physical appearance: faint yellow powder. Yield: 80%. Melting point: 186-190ºC. FT-IR: 1006.84 cm^{-1}, 1068.56 cm^{-1} (C-F stretching vibrations in the trifluoromethyl group), 1112.93 cm^{-1} (stretching vibrations attributed to the ether group), 1242.16 cm^{-1} (C-O stretching vibrations characteristic of the ester group), 1300.02 cm^{-1} (C-O stretching vibrations found in the carbamate group), 1373.32 cm^{-1} (C-H bending vibrations within the CH_3 group), 1508.33 cm^{-1}, 1541.12 cm^{-1} (C=C stretching vibrations typical of aromatic rings), 1683.86 cm^{-1} (C=O stretching vibrations in the carbamate carbonyl group), 1716.65 cm^{-1} (C=O stretching vibrations associated with the ester carbonyl group), 2939.52 cm^{-1}, 2976.16 cm^{-1} (asymmetric CH_3 stretching vibrations), and 3000 cm^{-1} (C-H stretching vibrations in aromatic rings). ^{1}H-NMR (DMSO-d_6, 400 MHz), δ (ppm): 1.03 – 1.04 (t, 6H, proton of CH_3), 2.13 (d, 3H, proton of CH_3), 2.29 (q, 1H, proton of CH_2), 2.43 (m, 2H, proton of CH_2), 2.83 – 2.86 (t, 2H, CH_2 attached to N atom), 4.81 (s, 3H, CH_3 attached to N atom), 5.66 (m, 1H, CH benzylic proton), 7.01 – 7.12 (d, 2H, CH proton of aromatic ring A), 7.28 – 7.30 (m, 2H, CH proton of aromatic ring B), 7.30 – 7.31 (t, 1H, CH of aromatic ring B), 7.36 – 7.38 (d, 2H, CH proton of aromatic ring B), 7.40 – 7.44 (t, 2H, CH of aromatic ring A), 7.46 – 7.58 (q, 2H, proton of O-CH-O).^{13}C-NMR (DMSO-d_6,100 MHz), δ(ppm):δ (ppm): 18.04 (CH_3, 2C), 20.72 (CH_3), 29.18 (CH_2), 29.51 (CH_2), 30.27 (CH_3), 44.57 (CH_2), 87.66 (CH-O), 92.08 (O-CH-O), 106.18 (C in aromatic ring A, 2C), 118.97 (C in aromatic ring A), 126.33 (C attached to the trifluoride group), 127.15 (CH in aromatic ring B), 128.13 (CH in aromatic ring A, 2C), 129.25 (CH in aromatic ring B, 2C), 133.20 (CH in aromatic ring B, 2C), 142.98 (C in aromatic ring B), 153.58 (C=O), 157.23 (C=O), 168.73 (C in aromatic ring).

Synthesis of compound (A4) (1S)-1-((methyl (3-phenyl-3-(4-(trifluoromethyl) phenoxy) propyl) carbamoyl) oxy) ethyl benzoate

Physical appearance: faint yellow sticky powder. Yield: 74%. Melting point 202-205ºC. FT-IR: 1029.99 cm^{-1} (C-F stretching vibrations in the CF_3 group), 1145.72 cm^{-1} (stretching vibrations attributed to the ether group), 1244.09 cm^{-1} (C-O stretching vibrations characteristic of the ester group), 1290.38 cm^{-1} (C-O stretching vibrations within the carbamate group), 1384.89 cm^{-1}, 1440.83 cm^{-1} (CH_3 group bending vibrations), 1608.63 cm^{-1} (C=C stretching vibrations typical of aromatic rings), 1645.28 cm^{-1} - 1700 cm^{-1} (C=O stretching vibrations corresponding to ester and carbamate groups), and 3230.77 cm^{-1} (C-H stretching vibrations in aromatic rings). ^{1}H-NMR (DMSO-d_6, 400 MHz), δ (ppm): 1.78 (d, 3H, proton of CH_3), 2.59 (m, 2H, proton of CH_2), 2.99 (t, 2H, CH_2 attached to N atom), 4.67 (s, 3H, CH_3 attached to N atom), 5.65 (t, 1H, CH of benzylic proton), 7.37 – 7.36 (d, 2H, CH proton of aromatic ring A), 7.41 – 7.46 (m, 2H, CH proton of aromatic ring B), 7.48 – 7.50 (t, 1H, CH proton of aromatic ring B), 7.57 (d, 2H, CH proton of aromatic ring B), 7.58 – 7.59 (t, 2H, CH proton of aromatic ring A), 7.61 (q, 2H, proton of O-CH-O), 7.91 (m, 2H, CH proton of aromatic ring C), 7.96 (t, 1H, CH proton of aromatic ring C), 7.97 – 7.98 (d, 2H, CH proton of aromatic ring C).^{13}C-NMR (DMSO-d_6, 100 MHz), δ (ppm): 12.30 (CH_3), 29.94 (CH_2), 34.19 (CH_3), 53.02 (CH_2), 81.54 (C), 86.06 (O-CH-O), 113.68 (CH in aromatic ring A, 2C), 117.92 (C in aromatic ring A), 121.28 (C connected to trifluoride), 123.63 (C in aromatic ring B), 126.79 (CH in aromatic ring A, 2C), 129.43 (CH in aromatic ring B, 2C), 131.32 (CH in aromatic ring B, 2C), 132.95 (CH in aromatic ring C, 2C), 136.00 (CH in aromatic ring C, 2C), 137.67 (C in aromatic ring C), 139.94 (CH in aromatic ring C), 140.29 (C in aromatic ring B), 147.44 (C=O), 156.47 (C in aromatic ring A), 162.47 (C=O).

Synthesis of compound (5A) (1S) 1((methyl (3phenyl3 (4(trifluoromethyl)phenoxy) propyl)carbamoyl)oxy)ethyl 2-hydroxybenzoate

Physical appearance: brown powder. Yield: 78%. Melting point: 290-294ºC. FT-IR: 1109.07 cm^{-1} (C-F stretching vibrations in the CF_3 group), 1157.29 cm^{-1} (stretching vibrations associated with the ether group), 1176.58 cm^{-1} (C-O stretching vibrations characteristic of the ester group), 1244.09 cm^{-1} (C-O stretching vibrations in the carbamate group), 1394.53 cm^{-1}, 1417.68 cm^{-1} (CH_3 group bending vibrations), 1519.91 cm^{-1}, 1541.12 cm^{-1} (C=C stretching vibrations typical of aromatic rings), 1683.86 cm^{-1} (C=O stretching vibrations in the carbamate group), 1697.36 - 1716.65 cm^{-1} (C=O stretching vibrations corresponding to the ester group), 2885.51 cm^{-1}, 2943.37 cm^{-1} (CH_3 group stretching vibrations), 3100 cm^{-1} (C-H stretching vibrations in aromatic rings), and 3311.78 cm^{-1} (phenolic OH stretching vibrations). ^{1}H-NMR (DMSO-d_6, 400 MHz), δ (ppm): 1.68 (d, 3H, proton of CH_3), 2.19 – 2.21 (m, 2H, proton of CH_2), 3.54 (t, 2H, CH_2 attached to N atom), 4.76 (s, 3H, CH_3 attached to N atom), 5.60 (t, 1H, CH proton of benzylic), 6.87 – 6.89 (d, 2H, CH proton of aromatic ring A), 6.91 – 6.94 (m, 2H, CH proton of aromatic ring C), 7.49 (m, 2H, CH proton of aromatic ring B), 7.57 (t, 1H, CH proton of aromatic ring B), 7.52 – 7.54 (t, 2H, CH proton of aromatic ring B), 7.56 (t, 1H, CH proton of aromatic ring C), 7.79 (d, 2H, CH proton of aromatic ring A), 7.81 (d, 1H, CH of aromatic ring C), 7.97 (q, 1H, O-CH-O proton), 10.91 (s, OH proton). ^{13}C-NMR (DMSO-d_6, 100 MHz), δ (ppm): 16.35 (CH_3), 27.44 (CH_2), 31.54 (CH_3), 56.08 (CH_2), 81.23 (CH), 95.29 (O-CH-O), 112.31 (C in aromatic ring B), 118.43 (CH in aromatic

ring A, 2C), 121.02 (CH in aromatic ring B connected to trifluoride), 123.01 (CH in aromatic ring B), 125.48 (C in aromatic ring A), 127.98 (C connected to trifluoride), 129.95 (CH in aromatic ring A, 2C), 131.26 (CH in aromatic ring C), 133.03 (CH in aromatic ring C, 2C), 134.47 (CH in aromatic ring C, 2C), 136.31 (CH in aromatic ring B), 140.34 (CH in aromatic ring B), 144.19 (C in aromatic ring C), 154.21 (C=O), 160.86 (C in aromatic ring A), 163.10 (C in aromatic ring B), 169.34 (C=O).

Enzymatic Hydrolysis

The enzymatic hydrolysis of the synthesized compounds (A1–A5) was conducted using human plasma (obtained from (Sigma-Aldrich, P9523) in powdered form was reconstituted according to the manufacturer's instructions and stored at 2–8°C). The plasma was diluted to approximately 80% with an isotonic phosphate buffer (pH 7.4) and maintained at 37 °C. To initiate the reaction, 5 mL of the heated plasma solution was added to 100 µL of the target compound stock solution. Samples were collected at specified intervals (15, 30, 60, and 120 minutes) and deproteinized with cold methanol. Hydrolysis rates were monitored using UV-Vis spectroscopy at λ_{max} = 227 nm after instant mixing and 5-minute centrifugation at 4,000 rpm [40].

Statistical Analysis

Statistical analysis was conducted to ensure the reliability and accuracy of the experimental data. All experiments were performed in triplicate, and the results are presented as mean ± standard deviation (SD). The mean and SD values were calculated using GraphPad Prism (version 9). One-way analysis of variance (ANOVA) was used to evaluate the differences in enzymatic hydrolysis rates among the various prodrug derivatives (A1–A5), allowing for the assessment of significant differences between the groups. A p-value of less than 0.05 was considered statistically significant [41]. Figure 1 represents hydrolysis percentages and their variability was generated using GraphPad Prism to ensure accurate visualization of trends and error margins.

Results and Discussion

FT-IR results

The first step in the formation of fluoxetine derivatives involves the reaction between a secondary amine and 1-chloroethyl chloroformate, resulting in the formation of a carbamate intermediate (R-NH-COOCH $(CH_3)Cl_2$) through a nucleophilic attack by the nitrogen of the amine on the carbonyl group. To confirm the successful formation of the prodrugs (A1–A5), FT-IR spectroscopy was employed by monitoring the absence of the N-H stretching band at 3300 cm^{-1}, which is characteristic of fluoxetine, and the appearance of a new C=O stretching band in the range of 1650–1700 cm^{-1}. This C=O band was a defining feature across all five derivatives and served as the standard to evaluate the success of the reaction through IR measurements S (1 to 5).

1H-NMR results

The A1-A5 compounds were characterized with 1HNMR to further confirm the identity of the final product (S6 to S10). Different patterns in distinctive proton signals were noted among the produced goods. The methyl group in molecule A1 generated a doublet at 1.71 ppm, suggesting a comparatively straightforward ester structure. For A2, a triplet for the methyl group at 0.94-0.95 ppm and a quartet for the adjacent CH_2 protons at 2.80-2.82 ppm indicate a more complex environment influenced by the ester group.

Compound A3 shows ester-related connectivity, with the methyl protons showing up as a triplet at 1.03–1.04 ppm and the CH_2 protons forming a quartet at 2.29 ppm. Aromatic proton signals are more intricate in compounds A4 and A5. At 7.91, 7.96, and 7.97-7.98 ppm, multiplets and triplets for the CH protons of aromatic ring C are observed in A4, suggesting substituent effects. A5 shows a triplet at 7.56 ppm and multiplet signals at 6.91-6.94 ppm, indicating further aromatic interactions. The hydroxyl proton in A5 at 10.91 ppm indicates significant deshielding, which could be caused by electron-withdrawing mechanisms or strong hydrogen bonding. The analysis of the ^{1}HNMR data, which demonstrates how the ester functional group influences the chemical environment of surrounding protons, confirms the structural identities of the generated compounds.

13C-NMR results

Compounds A1–A5 were further characterized by ^{13}C-NMR spectroscopy S (11 to 15) to validate their structures based on the characteristic carbon environments observed in their spectra. A1 exhibits a simple ester structure with a methyl carbon resonating at 16.35 ppm. A slightly more complex ester structure is indicated in A2, as evidenced by a CH_2 carbon at 27.44 ppm and a methyl carbon at 31.54 ppm. A3 shows characteristic ester carbons at 81.23 ppm (CH) and 95.29 ppm (O-CH-O), confirming its distinct structural features. For A4, aromatic carbons resonate in the range of 118–129 ppm, reflecting the substituent effects on the aromatic ring. In A5, the presence of downfield shifts at 154.21 ppm and 169.34 ppm for carbonyl carbons indicates strong electron-withdrawing interactions, consistent with the unique electronic environments in this compound.

Enzyme hydrolysis

In this study, the hydrolysis of five fluoxetine prodrug derivatives (A1–A5) was evaluated in human plasma to assess their potential for improving drug delivery and therapeutic outcomes. The results demonstrated that prodrug A1 exhibited the fastest hydrolysis rate, achieving a 99.5% conversion after 120 minutes, followed by A2 (97.0%), A3 (96.9%), A4 (95.0%), and A5 (94.5%). The differences in hydrolysis rates can be attributed to the varying steric properties of the acyloxyalkyl groups attached to each prodrug, which influence the interaction with esterases in human plasma. The A1 derivative, with a smaller and more flexible acyloxy group, showed optimal interaction with the enzymes, resulting in rapid hydrolysis. On the other hand, the larger or bulkier substituents on A2, A3, A4, and A5 introduced steric hindrance, leading to slower hydrolysis rates.

Table (2): Mean Percentage of hydrolysis with standard deviation of compounds over time.

Time (min)	A1 (%)	A2 (%)	A3 (%)	A4 (%)	A5 (%)
5	1.58±0.02	1.30±0.02	1.15±0.034	1.07±0.0578	0.94±0.09826
15	17.50±1.1	16.25±1.1	15.00±1.87	14.50±2.179	12.25±3.7043
30	26.00±1.3	24.75±1.3	23.25±2.21	22.25±2.757	19.50±3.3869
60	60.50±1.7	58.30±1.7	57.55±2.89	56.45±2.913	55.15±3.3521
120	99.50±2.5	97.00±2.5	96.90±2.25	95.00±3.225	94.50±3.2825

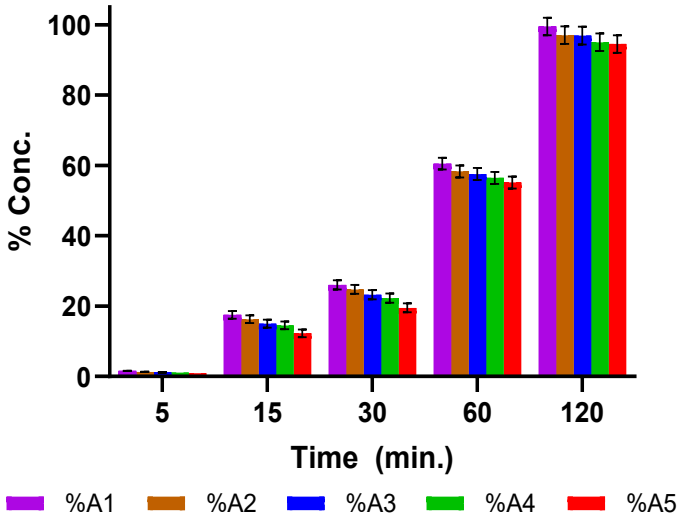

Figure (1): Mean percentage of hydrolysis rate of compounds (A1, A2, A3, A4 and A5). Error bars represent standard deviation (n=3).

Figure (1) visually represents the mean percentage hydrolysis rates of the compounds (A1–A5) over time (5, 15, 30, 60, and 120 minutes). The error bars represent the standard deviation (n = 3). The data show that all derivatives exhibited a progressive increase in hydrolysis percentage with time, reaching near-complete hydrolysis at 120 minutes. Notably, A1 consistently outperformed the other derivatives at every time point, aligning with its smaller acyloxyalkyl group and higher enzymatic affinity.

The hydrolysis of fluoxetine prodrugs in human plasma observed in the current study aligns closely with findings from prior research emphasizing the role of esterases in prodrug activation. For instance, Huttunen *et al*. (2018) identified carboxylesterase (CES) and paraoxonase (PON) as crucial enzymes in the hydrolysis of amino acid ester prodrugs of ketoprofen, supporting the observation that ester-linked prodrugs are efficiently bioconverted in plasma across different systems [42]. This validates the present study's findings, reinforcing the concept that esterases such as butyrylcholinesterase (BChE), CES, and PON play a central role in the controlled release of active compounds, enhancing the bioavailability and therapeutic efficacy of ester-containing prodrugs.

Similarly, Li *et al*. (2019) studied the esterase-mediated hydrolysis of simvastatin in human and rat blood, identifying CES and PON as the primary enzymes responsible for converting simvastatin to its active form, simvastatin acid [43]. The use of esterase inhibitors in their study demonstrated the substantial impact of hydrolysis on pharmacokinetic profiles, affecting both the concentration and bioavailability of the prodrug and its active metabolite. This finding parallels the importance of enzymatic activity in the current study, where the high conversion rates of fluoxetine prodrugs in plasma highlight the effectiveness of BChE-mediated hydrolysis in achieving optimal drug release.

Both the ketoprofen study by Huttunen *et al*. (2018) and the simvastatin study by Li *et al*. (2019) highlight the necessity of enzymatic hydrolysis for effective prodrug conversion. These insights complement the current study's findings, illustrating how the enzymatic activity of BChE ensures the efficient activation of fluoxetine prodrugs. This enzymatic process not only facilitates improved solubility and absorption but also addresses hepatic first-pass metabolism, ultimately enhancing the pharmacokinetic and pharmacodynamic profiles of the prodrugs.

By drawing parallels to these studies, the current research underscores the broader applicability of enzyme-mediated hydrolysis to various prodrugs, offering valuable insights into the design and development of novel prodrugs with enhanced therapeutic outcomes.

While this study provides valuable insights into the hydrolysis of fluoxetine prodrugs, several limitations should be acknowledged. One of the key limitations is the exclusive reliance on butyrylcholinesterase (BChE) for hydrolysis testing. Although BChE is a well-known enzyme for ester hydrolysis, it may not fully represent the diversity of enzymes involved in prodrug hydrolysis *in vivo*. Other esterases, such as carboxylesterases or cholinesterases, could contribute to prodrug activation in different tissues or under specific physiological conditions. Future studies should investigate the involvement of a broader range of esterases to better understand how prodrugs are hydrolyzed in various biological environments.

Moreover, this study was conducted in an *in vitro* setting using human plasma, which may not fully reflect the complexity of prodrug metabolism and pharmacokinetics *in vivo*. Factors such as enzyme expression levels, tissue-specific distribution, and absorption rates could influence the bioavailability and pharmacokinetics of the prodrugs in living organisms. *In vivo* studies are necessary to evaluate the pharmacokinetic profiles, toxicity, and therapeutic efficacy of these prodrugs in a more realistic biological context.

Finally, this study focused on a specific set of acyl groups for the prodrug derivatives. However, the selection of acyl groups may not encompass the full range of possible modifications that could impact hydrolysis rates and prodrug effectiveness. Future studies should explore a wider variety of acyl groups with larger or more diverse chemical structures to better understand how different modifications influence prodrug hydrolysis and therapeutic outcomes.

Several key areas of future research should be pursued to address this study's limitations and expand on the findings. First, the involvement of other esterases, such as carboxylesterases and cholinesterases, should be investigated to provide a more comprehensive understanding of prodrug hydrolysis *in vivo*. Exploring the contribution of tissue-specific esterases to prodrug activation could help elucidate the factors influencing prodrug bioavailability and release. Second, *in vivo* studies are essential for assessing the pharmacokinetics, bioavailability, and toxicity of fluoxetine prodrugs in living organisms. These studies will

provide valuable insights into how the prodrugs perform in more complex biological systems and help determine their therapeutic potential. Additionally, future research could focus on optimizing prodrug design through computational modeling and structure-activity relationship (SAR) analysis to predict the interaction of prodrugs with esterases and other enzymes.

Lastly, exploring alternative prodrug strategies, such as self-immolation prodrugs or nanoparticle-based drug delivery systems, could further enhance the controlled release and targeted delivery of fluoxetine. These approaches may offer additional benefits in improving drug efficacy, reducing side effects, and enabling site-specific drug release.

Conclusions

This study successfully synthesized and evaluated a series of fluoxetine derivatives (A1–A5) modified with acyloxyalkyl carbamate groups. The hydrolysis assays in human plasma demonstrated that drug release rates depended on the steric properties of the substituents, with A1 exhibiting the fastest hydrolysis. The results highlight the role of esterases, particularly butyrylcholinesterase, in prodrug activation, offering controlled release and enhanced bioavailability.Future studies should explore additional esterases, conduct *in vivo* assessments, and investigate alternative chemical modifications to optimize prodrug design. This research provides a strong foundation for developing fluoxetine prodrugs with improved therapeutic outcomes.

Open Access

References

1] Thapar A, Eyre O, Patel V, Brent D. Depression in young people. The Lancet. 2022;400(10352):617-31. DOI: 10.1016/S0140-6736(22)01012-1

2] Kalin, N.H. (2020). The critical relationship between anxiety and depression. American Journal of Psychiatry, 365-367. DOI.org/10.1176/appi.ajp.2020.20030305

3] Jeong HG, Lee HG, Lee JJ, Park SB, Huh JH, Han Y. Role of severity and gender in the association between late-life depression and all-cause mortality. Int Psychogeriatrics. 2013;25:677–84.DOI: 10.1017/S1041610212002190

4] Troubat R, Barone R, Leman P, Desmidt S, Cressant T, Atanasova A . Neuroinflammation and depression: A review. Eur J Neurosci. 2021;53:151–71.DOI.org/10.1111/ejn.14720

5] Troubat R, Barone P, Leman S, Desmidt T, Cressant A, Atanasova B. Neuroinflammation and depression: A review. European journal of neuroscience. 2021;53(1):151-71. DOI.org/10.1111/ejn.14720

6] Jesulola E, Micalos E, Baguley P. Understanding the pathophysiology of depression: From monoamines to the neurogenesis hypothesis model—are we there yet? Behav Brain Res. 2018;341:79–90.DOI.org/10.1016/j.bbr.2017.12.025

7] Maurer DM, Raymond TJ, Davis BN. Depression: screening and diagnosis. American family physician. 2018;98(8):508-15.

8] Edinoff AN, Akuly AN, Hanna HA, Ochoa TA, Patti CO, Ghaffar SJ. Selective serotonin reuptake inhibitors and adverse effects: a narrative review. Neurol Int. 2021;13:387–401.DOI.org/10.3390/neurolint13030038

9] Clevenger SS, Malhotra D, Dang J, Vanle B, IsHak WW. The role of selective serotonin reuptake inhibitors in preventing relapse of major depressive disorder. *Ther Adv Psychopharmacol.* 2018;8(1):49–58. https://doi.org/10.1177/2045125317737241.

10] .Nguyen TTL, *et al*. Selective serotonin reuptake inhibitor pharmaco-omics: mechanisms and prediction. Front Pharmacol. 2021;11:614048. DOI: 10.3389/fphar.2020.614048.

11] Edinoff AN, Akuly HA, Hanna TA, Ochoa CO, Patti SJ, Ghaffar YA. Selective serotonin reuptake inhibitors and adverse effects: a narrative review. Neurology international. 2021;13(3):387-401.DOI: 10.3390/neurolint13030038.

12] Gemmel M, Bögi E, Ragan C, Hazlett M, Dubovicky M, van den Hove DL. Perinatal selective serotonin reuptake inhibitor medication (SSRI) effects on social behaviors, neurodevelopment and the epigenome. Neuroscience & Biobehavioral Reviews. 2018;85:102-16.DOI: 10.1016/j.neubiorev.2017.04.023.

13] Almeida IB, Gomes IA, Shanmugam S, de Moura TR, Magalhães LS, de Aquino LAG. Inflammatory modulation of fluoxetine use in patients with depression: a systematic review and meta-analysis. Cytokine. 2020;131:155100.DOI: 10.1016/j.cyto.2020.155100

14] Ampuero E, Luarte A, Flores FS, Soto AI, Pino C, Silva V. The multifaceted effects of fluoxetine treatment on cognitive functions. Frontiers in Pharmacology. 2024;15:1412420.DOI: 10.3389/fphar.2024.1412420

15] Shelton RC. Serotonin and norepinephrine reuptake inhibitors. Antidepressants: From Biogenic Amines to New Mechanisms of Action. 2019:145-80.DOI: 10.1007/164_2018_164

16] Ampuero E, Luarte A, Flores FS, Soto AI, Pino C, Silva V. The multifaceted effects of fluoxetine treatment on cognitive functions. Front Pharmacol. 2024; 15:1412420.DOI: 10.3389/fphar.2024.1412420

17] Wang S-M, Han C, Bahk W-M, Lee S-J, Patkar AA, Masand PS .Addressing the side effects of contemporary antidepressant drugs: a comprehensive review. Chonnam Med J. 2018;54(2):101-12.DOI: 10.4068/cmj.2018.54.2.101

18] Markovic M, Ben-Shabat M, Keinan S, Aponick A, Zimmermann EM, Dahan A. Lipidic prodrug approach for improved oral drug delivery and therapy. Med Res Rev. 2019;39:579–607. DOI: 10.1002/med.21533.

19] Dakhil IA, Kadhim D, Mahdi ZH. An overview on the recent technologies and advances in drug delivery of poorly water-soluble drugs. Al Mustansiriyah J Pharm Sci. 2019;19(4):180–95.DOI.org/10.32947/ajps.v19i4.649

20] Mahdi MF, Dawood MF, Hussein AH. Design, synthesis and preliminary pharmacological evaluation of mutual prodrug of non-steroidal anti-inflammatory drugs coupling with natural

anti-oxidants via glycine. Al Mustansiriyah J Pharm Sci. 2013;13(1):155–69.DOI.org/10.32947/ajps.v13i1.211

21] Najjar A, Karaman R. The prodrug approach in the era of drug design. Expert opinion on drug delivery. 2019;16(1):1-5.DOI: 10.1080/17425247.2019.1553954.

22] Khazaal N, Taha N, Basim M, Amer H. Quick pharmaceutical steps for preliminary evaluation of a compound as a possible oral prodrug. Al Mustansiriyah J Pharm Sci. 2011;9(1):1–6.DOI.org/10.32947/ajps.v9i1.266

23] Sanches BM, Ferreira BM. Is prodrug design an approach to increase water solubility? Int J Pharm. 2019;568:118498.DOI: 10.1016/j.ijpharm.2019.118498

24] Rautio J, Meanwell NA, Di L, Hageman MJ. The expanding role of prodrugs in contemporary drug design and development. Nature reviews drug discovery. 2018;17(8):559-87.DOI: 10.1038/nrd.2018.46.

25] Markovic M, Ben-Shabat S, Keinan S, Aponick A, Zimmermann EM, Dahan A. Lipidic prodrug approach for improved oral drug delivery and therapy. Medicinal research reviews. 2019;39(2):579-607. DOI: 10.1002/med.21533

26] Gandhi PM, Chabukswar AR, Jagdale SC. Carriers for prodrug synthesis: A review. Indian J Pharm Sci. 2019;81(3):406-14.DOI:10.36468/pharmaceutical-sciences.524

27] Kalgutkar AS, Marnett AS, Crews AB, Remmel BC, Marnett RP. Ester and amide derivatives of the nonsteroidal anti-inflammatory drug, indomethacin, as selective cyclooxygenase-2 inhibitors. J Med Chem. 2000;43:2860–70. DOI: 10.1021/jm000004e

28] Alexander J, Cargill J, Michelson R, Schwam SR. (Acyloxy) alkyl carbamates as novel bioreversible prodrugs for amines: increased permeation through biological membranes. J Med Chem. 1988;31:318–22.DOI: 10.1021/jm00397a008

29] Gogate U, Repta U. N-(Acyloxyalkoxycarbonyl) derivatives as potential prodrugs of amines. I. Kinetics and mechanism of degradation in aqueous solutions. Int J Pharm. 1987;40:235–48.

30] Safadi M, Oliyai M, Stella R. Phosphoryloxymethyl carbamates and carbonates—novel water-soluble prodrugs for amines and hindered alcohols. Pharm Res. 1993;10:1350–5.DOI: 10.1023/a:1018934200343

31] Alexander J, Bindra J, Glass DS, Holahan JD, Renyer MA, Rork ML. Investigation of (oxodioxolenyl) methyl carbamates as nonchiral bioreversible prodrug moieties for chiral amines. J Med Chem. 1996;39:480–6.DOI: 10.1021/jm9506175

32] Mollica A, Feliciani A, Stefanucci F, Fadeev A, Pinnen EA. (Acyloxy) alkoxy moiety as amino acids protecting group for the synthesis of (R,R)-2,7-diaminosuberic acid via RCM. Protein Pept Lett. 2012;19:1245–9.DOI: 10.2174/092986612803521666

33] Gangwar S, Pauletti S, Siahaan GM, Stella TJ. Synthesis of a novel esterase-sensitive cyclic prodrug of a hexapeptide using an (acyloxy) alkoxy promoiety. J Org Chem. 1997;62:1356–62.

34] Bak B, Gudmundsson O, Gangwar S, Friis G, Siahaan T, Borchardt R. Synthesis and evaluation of the physicochemical properties of esterase-sensitive cyclic prodrugs of opioid peptides using an (acyloxy) alkoxy linker. J Peptide Res. 1999;53:393–402.DOI: 10.1034/j.1399-3011.1999.00070.x

35] Ghosh AK, Brindisi A. Organic carbamates in drug design and medicinal chemistry. J Med Chem. 2015;58:2895–940.DOI: 10.1021/jm501371s

36] Testa B, Mayer JM. Hydrolysis in drug and prodrug metabolism. John Wiley & Sons; 2003.

37] Alexander J. Process for preparing novel N-(acyloxy-alkoxy) carbonyl derivatives useful as bioreversible prodrug moieties for primary and secondary amine functions in drugs. Google Patents; 1990.

38] Bodor N. Prodrugs versus soft drugs. In: Bundgard H, editor. Design of Prodrugs. Elsevier; 1985.

39] Gogate U, Repta A. N-(Acyloxyalkoxycarbonyl) derivatives as potential prodrugs of amines. II. Esterase-catalyzed release of parent amines from model prodrugs. Int J Pharm. 1987;40:249–57.

40] Wadhwa LK, Sharma PD. Glycolamide ester of 6-methoxy-2-naphthylacetic acid as potential prodrugs—physicochemical properties, chemical stability and enzymatic hydrolysis. Int J Pharm. 1986;28:151–62.

41] Sahib MA, Mahdi MF. Molecular docking, synthesis, characterization, and preliminary evaluation of some new 3-ethyl-1H-indole derivatives as potential COX-2 inhibitors. *Adv J Chem Sect A.* 2025;8(5). DOI: 10.48309/ajca.2025.482848.1712.

42] Huttunen K. Identification of human, rat and mouse hydrolyzing enzymes bioconverting amino acid ester prodrug of ketoprofen. Bioorganic Chemistry. 2018;81:494-503.DOI: 10.1016/j.bioorg.2018.09.018

43] Li Z, Zhang J, Zhang Y, Zuo Z. Role of esterase mediated hydrolysis of simvastatin in human and rat blood and its impact on pharmacokinetic profiles of simvastatin and its active metabolite in rat. Journal of Pharmaceutical and Biomedical Analysis. 2019;168:13-22.DOI: 10.1016/j.jpba.2019.02.004